

LETTER TO THE EDITOR

## A study of the distant activity of comet C/2006 W3 (Christensen) with *Herschel* and ground-based radio telescopes<sup>★,★</sup>

D. Bockelée-Morvan<sup>1</sup>, P. Hartogh<sup>2</sup>, J. Crovisier<sup>1</sup>, B. Vandenbussche<sup>3</sup>, B. M. Swinyard<sup>4</sup>, N. Biver<sup>1</sup>, D. C. Lis<sup>5</sup>, C. Jarchow<sup>2</sup>, R. Moreno<sup>1</sup>, D. Hutsemékers<sup>6</sup>, E. Jehin<sup>6</sup>, M. Küppers<sup>11</sup>, L. M. Lara<sup>12</sup>, E. Lellouch<sup>1</sup>, J. Manfroid<sup>6</sup>, M. de Val-Borro<sup>2</sup>, S. Szutowicz<sup>7</sup>, M. Banaszekiewicz<sup>7</sup>, F. Bensch<sup>8</sup>, M. I. Blecka<sup>7</sup>, M. Emprechtinger<sup>5</sup>, T. Encrenaz<sup>1</sup>, T. Fulton<sup>9</sup>, M. Kidger<sup>10</sup>, M. Rengel<sup>2</sup>, C. Waelkens<sup>3</sup>, E. Bergin<sup>13</sup>, G. A. Blake<sup>5</sup>, J. A. D. L. Blommaert<sup>3</sup>, J. Cernicharo<sup>14</sup>, L. Decin<sup>3</sup>, P. Encrenaz<sup>15</sup>, T. de Graauw<sup>16,17,18</sup>, S. Leeks<sup>4</sup>, A. S. Medvedev<sup>2</sup>, D. Naylor<sup>19</sup>, R. Schieder<sup>20</sup>, and N. Thomas<sup>21</sup>

(Affiliations are available in the online edition)

Received 31 March 2010 / Accepted 7 May 2010

### ABSTRACT

Comet C/2006 W3 (Christensen) was observed in November 2009 at 3.3 AU from the Sun with *Herschel*. The PACS instrument acquired images of the dust coma in 70- $\mu\text{m}$  and 160- $\mu\text{m}$  filters and spectra covering several H<sub>2</sub>O rotational lines. Spectra in the range 450–1550 GHz were acquired with SPIRE. The comet emission continuum from 70 to 672  $\mu\text{m}$  was measured, but no lines were detected. The spectral energy distribution indicates thermal emission from large particles and provides a measure of the size distribution index and dust production rate. The upper limit to the water production rate is compared to the production rates of other species (CO, CH<sub>3</sub>OH, HCN, H<sub>2</sub>S, OH) measured with the IRAM 30-m and Nançay telescopes. The coma is found to be strongly enriched in species more volatile than water, in comparison to comets observed closer to the Sun. The CO to H<sub>2</sub>O production rate ratio exceeds 220%. The dust-to-gas production rate ratio is on the order of 1.

**Key words.** comets: individual: C/2006 W3 (Christensen) – techniques: photometric – radio lines: planetary systems – radio continuum: planetary systems – comets: general

### 1. Introduction

Direct imaging shows that distant activity is a general property of cometary nuclei (e.g., Mazzotta Epifani et al. 2009). It is attributed to the sublimation of hypervolatile ices, such as CO or CO<sub>2</sub>, or to the release of volatile species trapped in amorphous water ice during the amorphous-to-crystalline phase transition (Prialdnik et al. 2004). Indeed, at heliocentric distances  $r_h$  larger than 3–4 AU, the sublimation of water, the major volatile in cometary nuclei, is inefficient. Characterizing the processes responsible for distant activity is important for understanding the structure and composition of cometary nuclei, their thermal properties and their evolution upon solar heating. However, detailed investigations of distant nuclei are sparse. The best studied objects are the distant comet 29P/Schwassmann-Wachmann 1, where CO, CO<sup>+</sup>, and CN were detected at 6 AU from the Sun, and C/1995 O1 (Hale-Bopp), whose exceptional activity allowed us to detect several molecules and radicals farther than 3 AU – including CO up to 14 AU (Biver et al. 2002; Rauer et al. 2003).

Comet C/2006 W3 (Christensen) was discovered in November 2006 at  $r_h = 8.6$  AU from the Sun with a total visual magnitude  $m_v \sim 18$ . This long-period comet passed

perihelion on July 6, 2009 at  $r_h = 3.13$  AU. Because of its significant brightness ( $m_v \sim 8.5$  at perihelion), it was an interesting target for the study of distant cometary activity. We report here on observations undertaken at  $r_h = 3.3$  AU post-perihelion with the PACS (Poglitsch et al. 2010) and SPIRE (Griffin et al. 2010) instruments on *Herschel* (Pilbratt et al. 2010), in the framework of the *Herschel* guaranteed time key project called “Water and related chemistry in the Solar System” (Hartogh et al. 2009). These observations are complemented by production rate measurements of several species with the Nançay radio telescope and the 30-m telescope of the Institut de Radioastronomie millimétrique (IRAM) at 3.2–3.3 AU pre- and post-perihelion.

### 2. Observations with *Herschel*

Comet C/2006 W3 (Christensen) was observed with *Herschel* on November 1–8, 2009 at  $r_h \sim 3.3$  AU and a distance from *Herschel*  $\Delta = 3.5$ –3.7 AU.

There were two PACS observations acquired during the *Herschel* science demonstration phase: on November 1.83 UT, simultaneous acquisition of 8'  $\times$  11' coma images (Fig. 1) in blue (60–85  $\mu\text{m}$ ) and red (130–210  $\mu\text{m}$ ) bands with the scan map photometry mode with a scan speed of 10"/sec (Obsid #1342186621 and 1342186622 with orthogonal scanning, duration  $t_{\text{int}} = 565$  s each), and on November 8.74–8.82 UT, pointed source dedicated line spectroscopy over a 47"  $\times$  47" field of view (5  $\times$  5 pixels of 9.4") with a large (6') chopper throw and a number (so-called line repetition  $l_{\text{rep}}$ ) of ABBA nodding

\* *Herschel* is an ESA space observatory with science instruments provided by European-led Principal Investigator consortia and with important participation from NASA.

\*\* Figures 2, 5, 6 are only available in electronic form at <http://www.aanda.org>

**Table 1.** Molecular observations in comet C/2006 W3 (Christensen).

	2009 UT date [mm/dd.dd]	$\langle r_h \rangle$ [AU]	$\langle \Delta \rangle$ [AU]	Line	Intensity	Unit	Velocity shift [km s <sup>-1</sup> ]	Prod. rate [s <sup>-1</sup> ]
PACS	11/8.74–8.82	3.35	3.70	H <sub>2</sub> O(2 <sub>12</sub> –1 <sub>01</sub> ) <sup>a</sup>	$<2.2 \times 10^{-18a}$	W m <sup>-2</sup>	–	$<1.4 \times 10^{28}$
SPIRE	11/6.59–6.68	3.34	3.65	H <sub>2</sub> O(1 <sub>11</sub> –0 <sub>00</sub> )	$<8 \times 10^{-18}$	W m <sup>-2</sup>	–	$<4 \times 10^{28}$
Nançay	02/10–04/19	3.27	3.90	OH 18 cm	$-0.016 \pm 0.003$	Jy km s <sup>-1</sup>	$-0.32 \pm 0.12$	$3.8 \pm 0.9 \times 10^{28}$
IRAM	09/13.88	3.20	2.57	HCN(1–0)	$0.271 \pm 0.015$	K km s <sup>-1b</sup>	$-0.21 \pm 0.03$	$1.6 \pm 0.1 \times 10^{26}$
	09/13.93	3.20	2.57	HCN(3–2)	$0.961 \pm 0.140$		$-0.15 \pm 0.06$	$1.8 \pm 0.3 \times 10^{26}$
	09/14.86	3.20	2.59	HCN(1–0)	$0.262 \pm 0.013$		$-0.10 \pm 0.03$	$1.6 \pm 0.1 \times 10^{26}$
	09/14.93	3.20	2.59	HCN(3–2)	$0.972 \pm 0.097$		$+0.03 \pm 0.04$	$1.6 \pm 0.2 \times 10^{26}$
	09/14.88	3.20	2.59	CO(2–1)	$0.433 \pm 0.028$		$-0.04 \pm 0.03$	$3.9 \pm 0.3 \times 10^{28}$
	09/14.40	3.20	2.58	CH <sub>3</sub> OH(1 <sub>0</sub> –1 <sub>-1</sub> E) <sup>c</sup>	$0.086 \pm 0.011$		$-0.10 \pm 0.04$	$1.5 \pm 0.3 \times 10^{27}$
	09/14.93	3.20	2.59	H <sub>2</sub> S(1 <sub>10</sub> –1 <sub>01</sub> )	$0.311 \pm 0.031$		$-0.05 \pm 0.04$	$1.0 \pm 0.1 \times 10^{27}$
	09/14.95	3.20	2.59	CS(2–1)	$0.028 \pm 0.012$		–	$0.5 \pm 0.2 \times 10^{26}$
	09/14.95	3.20	2.59	H <sub>2</sub> CO(3 <sub>12</sub> –2 <sub>11</sub> )	$<0.203$		–	$<1 \times 10^{27}$
	10/29.71	3.32	3.48	HCN(1–0)	$0.165 \pm 0.010$		$-0.15 \pm 0.03$	$1.4 \pm 0.1 \times 10^{26}$
	10/29.71	3.32	3.48	CO(2–1)	$0.248 \pm 0.026$		$-0.11 \pm 0.03$	$3.0 \pm 0.3 \times 10^{28}$

**Notes.** <sup>(a)</sup>  $3\text{-}\sigma$  upper limit per pixel in the central  $9.4'' \times 9.4''$  pixel. The upper limit on the flux per beam is estimated to be  $\sim 2$  times higher. Upper limits for H<sub>2</sub>O 2<sub>21</sub>–1<sub>10</sub>, 3<sub>13</sub>–2<sub>02</sub>, 2<sub>21</sub>–2<sub>12</sub>, and 3<sub>03</sub>–2<sub>12</sub> lines are 4.9, 1.8, 1.0, and 3.9 ( $\times 10^{-18}$ ) W m<sup>-2</sup> respectively. <sup>(b)</sup> For IRAM data, the intensity scale is the main beam brightness temperature. <sup>(c)</sup> CH<sub>3</sub>OH 2<sub>0</sub>–2<sub>-1</sub>E, 3<sub>0</sub>–3<sub>-1</sub>E, 4<sub>0</sub>–4<sub>-1</sub>E, 5<sub>0</sub>–5<sub>-1</sub>E, and 6<sub>0</sub>–6<sub>-1</sub>E lines were also observed with line intensities of 0.083, 0.062, 0.049, 0.043, and 0.022 ( $\pm 0.010$ ) K km s<sup>-1</sup>, respectively.

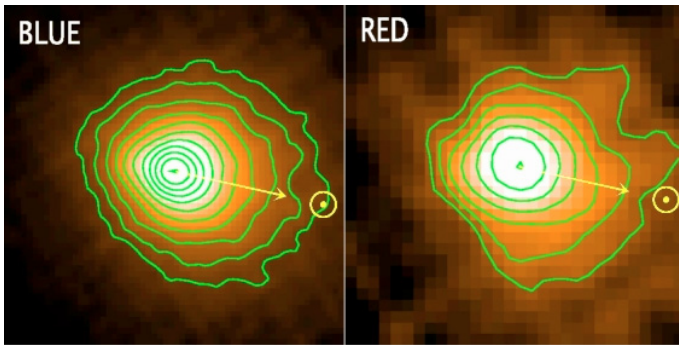


**Fig. 1.** Blue (70  $\mu\text{m}$ ) and red (160  $\mu\text{m}$ )  $1' \times 1'$  maps of C/2006 W3 (Christensen) observed with PACS on November 1, 2009 UT. The pixel size is  $1''$  in the blue map and  $2''$  in the red map. Contour levels are stepped by 0.1 in Log, up to 99% of maximum intensity. East is on the left, North is up. The Sun direction is indicated.

cycles (Obsid #1342186633,  $t_{\text{int}} = 6837$  s). The water lines 2<sub>21</sub>–1<sub>10</sub> (108.07  $\mu\text{m}$ ,  $l_{\text{rep}} = 2$ ), 3<sub>13</sub>–2<sub>02</sub> (138.53  $\mu\text{m}$ ,  $l_{\text{rep}} = 2$ ), 3<sub>03</sub>–2<sub>12</sub> (174.63  $\mu\text{m}$ ,  $l_{\text{rep}} = 3$ ), 2<sub>12</sub>–1<sub>01</sub> (179.53  $\mu\text{m}$ ,  $l_{\text{rep}} = 1$ ) and 2<sub>21</sub>–2<sub>12</sub> (180.49  $\mu\text{m}$ ,  $l_{\text{rep}} = 1$ ) were targeted at a spectral resolution  $\Delta\lambda \sim 0.11\text{--}0.12$   $\mu\text{m}$ . The PACS data were processed with the HIPE software version 2.3.1, which uses ground calibration for the signal-to-flux conversion. A high-pass filter with a width of 297 was used to remove the  $1/f$  noise. According to sky calibration sources, PACS spectroscopy fluxes in the 100–220  $\mu\text{m}$  range are too high by a factor of 1.1 on average, with a 30% accuracy. For the blue and red maps, the overestimation factors are 1.05 and 1.29, and the flux accuracies are 10 and 20%, respectively. We applied these corrections. No hint of lines is present in the PACS spectra (*online* Fig. 2, Table 1 for upper limits). However, thermal emission from the dust coma is detected in the 25 pixels.

On November 6.59–6.68 UT the comet was observed using the central pixels on the SPIRE spectrometer for a total duration of 6926 s. The spectral range (450–1550 GHz) encompasses the fundamental ortho 1<sub>10</sub>–1<sub>01</sub> and para 1<sub>11</sub>–0<sub>00</sub> water lines. This source was extremely faint for the SPIRE spectrometer. Standard pipeline reduction showed significant problems with the overall flux level in both the high- (SSW) and low- (SLW) frequency channels. A different approach has been taken therefore, which does not rely on the standard pipeline processing. It uses the

variation in bolometer temperature to transform the source and dark interferograms into spectra, which are then subtracted and divided by a calibration spectrum obtained on a bright source (Uranus).

Another aspect that is not currently accurately calibrated in standard processing is the effect of variations in the instrument temperature between the observation of the dark sky and the source: this can cause large relative variations in the recorded spectrum in the low frequency SLW portion. For the data presented here we determined the overall net flux of the source with no subtraction or addition of flux from the variation in instrument temperature. We then inspected the low frequency spectrum and compared it to the spectrum expected from the subtraction of two black bodies at temperatures given by the average instrument temperatures recorded in the housekeeping data. In general, as with the standard pipeline, this gives either too much or too little flux and a non-physical spectrum compared to the spectrum seen in the (unaffected) high-frequency band. The difference in model instrument temperatures in the dark sky and the source observation were therefore varied until a match between the overall flux level in SSW was achieved and the flux at the lowest frequencies is zero within the noise. The degree of variation in the temperature difference required to achieve this is less than 1% of the recorded temperatures.

The comet is somewhat extended in the beam of the SPIRE spectrometer, so a correction is required to the shape of the spectrum to account for the varying beam size of the instrument with frequency (Swinyard et al. 2010). We normalised this correction here to give the flux in an effective beam size of 18.7'' for both the SSW and SLW channels. Inspection of the data shows that no line is detected within a  $3\text{-}\sigma$  upper limit of  $0.7\text{--}0.8 \times 10^{-17}$  W m<sup>-2</sup>. Continuum emission from the coma is detected (Fig. 3).

### 3. Observations with ground-based telescopes

The OH lines at 18 cm were observed in comet C/2006 W3 (Christensen) with the Nançay radio telescope (Fig. 4, Table 1). The methods of observation and analysis are described in Crovisier et al. (2002). The observations were done pre-perihelion from February 10 to April 19, 2009 when the comet was at an average heliocentric distance similar to that of the

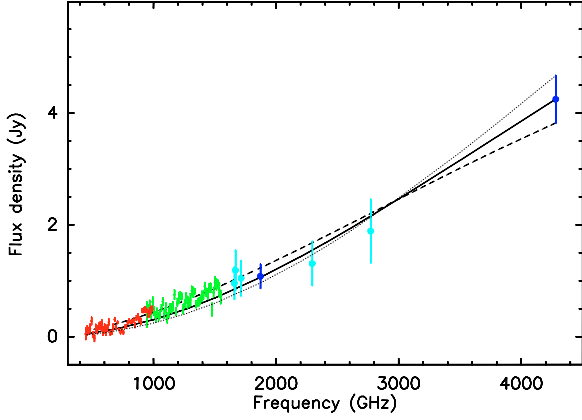


**Fig. 3.** Spectral energy distribution of C/2006 W3 (Christensen) combining SPIRE (SLW: red dots; SSW: green dots), PACS photometry (blue dots), and spectroscopy (cyan dots) data, scaled to a half power beam width of  $18.7''$  and  $\Delta = 3.65$  AU. The SPIRE data were binned from  $\sim 0.02$  to  $0.4$   $\text{cm}^{-1}$ . Curves are models for amorphous carbon grains with  $a_{\text{max}} = 0.9$  mm, and size index  $-3.6$  (solid),  $-2.8$  (dashed), and  $-3.85$  (dotted) (see text).

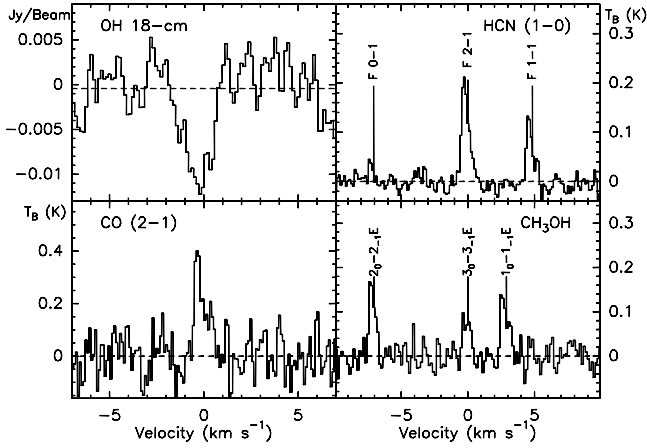


**Fig. 4.** Sample of ground-based spectra of comet C/2006 W3 (Christensen) acquired in 2009: OH spectrum (average of 1665 and 1667 MHz lines) observed at Nançay on Feb. 2 to Apr. 19, and HCN (Sept. 13–14), CO (Oct. 29), and CH<sub>3</sub>OH (Oct. 14) spectra observed at the IRAM-30m.

*Herschel* post-perihelion observations. An average OH production rate  $Q_{\text{OH}} = 3.8 \pm 0.9 \times 10^{28} \text{ s}^{-1}$  was derived, which corresponds to a water production rate  $Q_{\text{H}_2\text{O}} = 1.1 \times Q_{\text{OH}} = 4.2 \pm 1.0 \times 10^{28} \text{ s}^{-1}$ , assuming that water is the main source of OH radicals.

Observations with the IRAM 30-m were made on September 12–14, 2009 with the recently installed EMIR receiver, completed by a short observation on October 29 just before the *Herschel* observations (Fig. 4 and *online* Fig. 5, Table 1). CO, HCN (two rotational transitions), CH<sub>3</sub>OH (six lines around 157 GHz) and H<sub>2</sub>S were detected. Beam sizes are between 10 and  $27''$ , similar to PACS and SPIRE fields of view.

#### 4. Analysis and discussion

The observed water rotational lines are optically thick (e.g., Biver et al. 2007; Hartogh et al. 2010). To derive upper limits for the water production rate, we used an excitation model which considers radiation trapping, excitation by collisions with neutrals (here CO) and electrons, and solar IR pumping (Biver 1997; Biver et al. 1999). An H<sub>2</sub>O-CO total cross-section for de-excitation of  $2 \times 10^{-14} \text{ cm}^2$  is assumed (Biver et al. 1999). The

same excitation processes are considered in the models used to analyze the molecular lines observed at the IRAM 30-m. We used a gas kinetic temperature of 18 K, derived from the relative intensities of the CH<sub>3</sub>OH lines, and a gas expansion velocity of  $0.47 \text{ km s}^{-1}$ , consistent with the widths of lines detected at IRAM. The largest model uncertainty is in the electron density profile. We used the profile derived from the 1P/Halley in-situ measurements and scaled it to the heliocentric distance and activity of comet Christensen, as detailed in e.g. Bensch & Bergin (2004). The electron density was then multiplied by a factor  $x_{\text{ne}} = 0.2$ , constrained from observations of the 557 GHz water line in other comets (Biver et al. 2007; Hartogh et al. 2010). Upper limits on the water production rate obtained from the  $2_{12}-1_{01}$  line observed with PACS, and from the  $1_{11}-0_{00}$  line observed with SPIRE, are given in Table 1. Other observed H<sub>2</sub>O lines, either with PACS or with SPIRE do not improve these limits. The higher water production rate measured pre-perihelion at Nançay may suggest a seasonal effect. As the field of view of the Nançay telescope is large ( $3.5' \times 19'$ ), another interpretation is the detection of water sublimating from icy grains. The  $Q(\text{H}_2\text{O})$  measured at Nançay corresponds to a sublimation cross-section of  $400 \text{ km}^2$ , or a sublimating sphere of pure ice of 8 km radius.

With a CO production rate of  $3 \times 10^{28} \text{ s}^{-1}$ , comet Christensen is only four times less productive than comet Hale-Bopp at  $r_{\text{h}} = 3.3$  AU (Biver et al. 2002). The post-perihelion measurements show that the CO to H<sub>2</sub>O production rate ratio in comet Christensen exceeds 220%, indicating a CO-driven activity (Table 1). For comparison, CO/H<sub>2</sub>O was  $\sim 120\%$  in comet Hale-Bopp at 3.3 AU from the Sun. When normalized to HCN, abundance ratios HCN:CO:CH<sub>3</sub>OH:H<sub>2</sub>S:CS are 1:240:9:6:0.3 and 1:150:10:9:0.3 for comets Christensen and Hale-Bopp, respectively (*online* Fig. 6, Biver et al. 2002). Therefore, besides being depleted in H<sub>2</sub>O, comet Christensen is enriched in CO relative to HCN, while other molecules have similar abundances.

The dust coma is highly condensed but clearly resolved in both blue (B) and red (R) PACS images (Fig. 1). The width at half maximum of the radial profiles is  $9.0''$  and  $18.1''$  in B and R, respectively, a factor 1.64 larger than the PSF ( $\sim 5.5''$  in B,  $11''$  in R). The B image is extended westward towards the Sun direction at PA =  $257.5^\circ$  (phase angle =  $16^\circ$ ). This asymmetry is also seen in the R image. HCN and CO spectral lines are similarly blue-shifted (Table 1), which indicates preferentially day-side emission of these molecules from the nucleus, and is consistent with the dust coma morphology. Because CO is likely the main escaping gas (CO<sub>2</sub> has been observed to be less abundant than CO in comets, Bockelée-Morvan et al. 2004), dust-loading by CO gas is suggested. The enhanced CO production towards the Sun implies sub-surface production at depths not exceeding the thermal skin depth ( $\leq 1$  cm). The distant CO production in comet Christensen may result from the crystallization of amorphous water ice immediately below the surface (Priyalnik et al. 2004).

Radial profiles in the B and R bands are presented in Fig. 7 for both the comet and the PSF (from Vesta data). Although highly structured, the background was estimated as best as possible and subtracted. The PSF has a complex shape, which was fitted radially with two Gaussian profiles centered at  $\rho = 0$  and  $\rho = 6''$  (resp.  $12''$ ) for the B (resp. R) bands. A symmetric 2D PSF was then constructed and convolved with theoretical cometary surface brightness profiles  $S_{\text{B}} \propto \rho^{-x}$ . One finds that the full range of radial profiles can be reproduced with  $0.8 < x < 1.2$ . Most of the dispersion is likely due to the PSF structure and more specifically to its extended tri-lobe pattern (Lutz 2010). The average surface brightness profiles can be fitted with

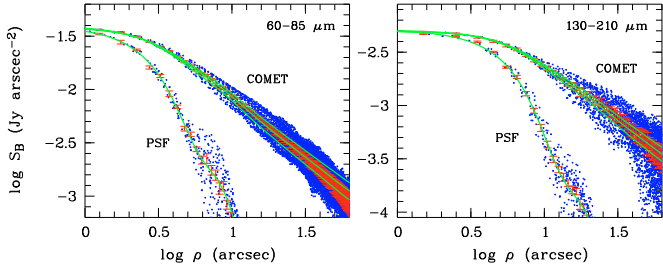


**Fig. 7.** Comet surface brightness and re-scaled PSF (Vesta) in B (left box) and R (right box) bands. Blue dots: surface brightness for each pixel. Red dots: mean values in 0.5'' (B) or 1.0'' (R) wide annuli, with error bars. For the comet the continuous green lines are radial profiles obtained by convolving a  $\rho^{-x}$  law with the PSF with, from top to bottom,  $x = 1.0, 1.05, 1.1$  (B) and  $x = 0.95, 1.0, 1.05$  (R). The green line superimposed on Vesta data is the PSF model (see text).

$x = 1.05 \pm 0.05$  in the B band and  $x = 1.00 \pm 0.05$  in the R band. The radial dependence of the surface brightness is then compatible with the steady-state  $\rho^{-1}$  law in the full 60–210  $\mu\text{m}$  spectral range.

There is then no evidence for a significant contribution of nucleus thermal emission in the central pixels. Assuming that the CO production rate scales proportionally to the nucleus surface area, the size of Christensen's nucleus is estimated to be a factor of two smaller than Hale-Bopp's nucleus size, i.e.  $D \sim 20$  km for comet Christensen (see Altenhoff et al. 1999, for Hale-Bopp's nucleus size). From the Standard Thermal Model (Lebofsky & Spencer 1989) with the nucleus albedo set to 4% and the emissivity and beaming factor taken as unity, a 20 km diameter body would contribute to 4.5% of the flux measured in the central 1'' pixel of the B image ( $F_B = 38.4$  mJy/pixel), and still less (2%) in the R image where the measured peak intensity is  $F_R = 19.5$  mJy/pixel (2''-pixel). From the B image we estimated that  $D < 26$  km.

The spectral energy distribution (SED) of the dust thermal emission can constrain important properties of cometary dust, in particular the dust size distribution and production rate (Jewitt & Luu 1990). The flux density in the SPIRE spectrum (Fig. 3) varies as  $\nu^{-1.78}$ . The spectral index, close to  $\alpha = 2$ , indicates the presence of large grains, consistent with the maximum ejectable dust size loaded by the CO gas ( $a_{\text{max}} \sim 0.9$  mm for a  $D = 20$  km body of density  $\rho_N = 500$  kg m $^{-3}$ , with the dust density  $\rho_d = \rho_N$ ;  $a_{\text{max}} \propto D^{-3}$ ; Crifo et al. 2005). We modeled the thermal emission of the dust coma following Jewitt & Luu (1990). Absorption cross-sections calculated with the Mie theory were used to compute both the temperature of the grains, solving the equation of radiative equilibrium, and their thermal emission. Complex refractive indices of amorphous carbon and olivine (Mg:Fe = 50:50) (Edoh 1983; Dorschner et al. 1995) were taken as broadly representative of cometary dust. We considered a differential dust production  $Q_d(a)$  as a function of size, with sizes between 0.1  $\mu\text{m}$  and 0.9 mm. The size-dependent grain velocities  $v_d(a)$  were computed following Crifo & Rodionov (1997) assuming  $D = 20$  km, and vary from 6 to 224 m s $^{-1}$  ( $\propto a^{-0.5}$  at large sizes). We assumed a local dust density  $\propto r^{-2}$ , where  $r$  is the distance to the nucleus, consistent with the maps. The best fit to the flux ratio  $F_B/F_R$  in R and B bands is obtained for  $Q_d(a) \propto a^{-(3.6^{+0.25}_{-0.8})}$ , which yields a dust opacity (the ratio between the effective emitting dust cross-section and dust mass), of  $6.8^{+1.2}_{-2.8}$  and  $5.7^{+0.3}_{-1.3}$  m $^2$  kg $^{-1}$  at 450 GHz, and dust production rates of

$850^{+1100}_{-200}$  and  $920^{+730}_{-110}$  kg s $^{-1}$ , for carbon and olivine grains, respectively. The whole SED between 450 and 4300 GHz is consistently explained (Fig. 3). Assuming that CO is the main gas escaping from the nucleus, the inferred dust-to-gas mass production ratio is then 0.5 to 1.4.

## 5. Conclusions

Comet Christensen was a distant comet. Nevertheless, the continuum was clearly detected by PACS and SPIRE, providing useful constraints on the properties of the cometary dust. Although water emission was not detected in this object, the limits obtained are significant. The prospects for future cometary studies with *Herschel* are thus very good.

*Acknowledgements.* PACS has been developed by a consortium of institutes led by MPE (Germany) and including UVIE (Austria); KU Leuven, CSL, IMEC (Belgium); CEA, LAM (France); MPIA (Germany); INAF-IFSI/OAA/OAP/OAT, LENS, SISSA (Italy); IAC (Spain). This development has been supported by the funding agencies BMVIT (Austria), ESA-PRODEX (Belgium), CEA/CNES (France), DLR (Germany), ASI/INAF (Italy), and CICYT/MCYT (Spain). SPIRE has been developed by a consortium of institutes led by Cardiff University (UK) and including Univ. Lethbridge (Canada); NAOC (China); CEA, LAM (France); IFSI, Univ. Padua (Italy); IAC (Spain); Stockholm Observatory (Sweden); Imperial College London, RAL, UCL-MSSL, UKATC, Univ. Sussex (UK); and Caltech, JPL, NHSC, Univ. Colorado (USA). This development has been supported by national funding agencies: CSA (Canada); NAOC (China); CEA, CNES, CNRS (France); ASI (Italy); MCINN (Spain); Stockholm Observatory (Sweden); STFC (UK); and NASA (USA). Additional funding support for some instrument activities has been provided by ESA. HCSS/HSpot/HIPE are joint developments by the *Herschel* Science Ground Segment Consortium, consisting of ESA, the NASA *Herschel* Science Center, and the HIFI, PACS and SPIRE consortia. IRAM is an international institute co-funded by CNRS, France, MPG, Germany, and IGN, Spain. The Nançay radio observatory is co-funded by CNRS, Observatoire de Paris, and the Région Centre (France). D.B.-M. thanks M.A.T. Groenewegen and D. Ladjal for support in PACS data analysis, and V. Zakharov for useful discussions on gas and dust dynamics.

## References

- Altenhoff, W. J., Biegging, J. H., Butler, B., et al. 1999, A&A, 348, 1020  
 Bensch, F., & Bergin, E. A. 2004, ApJ, 615, 531  
 Biver, N. 1997, PhD Thesis, Université Denis Diderot, Paris  
 Biver, N., Bockelée-Morvan, D., Colom, P., et al. 2002, Earth Moon and Planets, 90, 5  
 Biver, N., Bockelée-Morvan, D., Crovisier, J., et al. 1999, AJ, 118, 1850  
 Biver, N., Bockelée-Morvan, D., Crovisier, J., et al. 2007, P&SS, 55, 1058  
 Bockelée-Morvan, D., Crovisier, J., Mumma, M. J., & Weaver, H. A. 2004, in Comets II, ed. M. C. Festou, H. U. Keller, & H. A. Weaver (Tucson: The University of Arizona Press), 391  
 Crifo, J. F., & Rodionov, A. V. 1997, Icarus, 127, 319  
 Crifo, J.-F., Loukianov, G. A., Rodionov, A. V., & Zakharov, V. V. 2005, Icarus, 176, 192  
 Crovisier, J., Colom, P., Gérard, E., Bockelée-Morvan, D., & Bourgois, G. 2002, A&A, 393, 1053  
 Dorschner, J., Begemann, B., Henning, T., Jaeger, C., & Mutschke, H. 1995, A&A, 300, 503  
 Edoh, J. H. 1983, PhD Thesis, University of Arizona  
 Griffin, M. J. et al., 2010, A&A, 518, L3  
 Hartogh, P., Lellouch, E., Crovisier, J., et al. 2009, P&SS, 57, 1596  
 Hartogh, P., et al. 2010, A&A, 518, L150  
 Jewitt, D., & Luu, J. 1990, ApJ, 365, 738  
 Lebofsky, L. A., & Spencer, J. R. 1989, in Asteroids II, ed. R. P. Binzel, T. Gehrels, & M. S. Matthews (Tucson: The University of Arizona Press), 128  
 Lutz, D. 2010, PACS photometer point spread function, PACC-ME-TN-033  
 Mazzotta Epifani, E., Palumbo, P., & Colangeli, L. 2009, A&A, 508, 1031  
 Pilbratt, G. L. et al. 2010, A&A, 518, L1  
 Poglitsch, A. et al., 2010, A&A, 518, L2  
 Rauer, H., Helbert, J., Arpigny, C., et al. 2003, A&A, 397, 1109  
 Swinyard, B. M., et al. 2010, A&A, 518, L4  
 Pralnik, D., Benkhoff, J., & Podolak, M. 2004, in Comets II, ed. M. C. Festou, H. U. Keller, & H. A. Weaver (Tucson: The University of Arizona Press), 359

- 
- <sup>1</sup> LESIA, Observatoire de Paris, 5 place Jules Janssen, 92195 Meudon, France  
e-mail: dominique.bockelee@obspm.fr
- <sup>2</sup> Max-Planck-Institut für Sonnensystemforschung, Katlenburg-Lindau, Germany
- <sup>3</sup> Instituut voor Sterrenkunde, Katholieke Universiteit Leuven, Belgium
- <sup>4</sup> Rutherford Appleton Laboratory, Oxfordshire, UK
- <sup>5</sup> California Institute of Technology, Pasadena, USA
- <sup>6</sup> F.R.S.-FNRS, Institut d'Astrophysique et de Géophysique, Liège, Belgium
- <sup>7</sup> Space Research Centre, Polish Academy of Science, Warszawa, Poland
- <sup>8</sup> Deutsches Zentrum für Luft- und Raumfahrt (DLR), Bonn, Germany

- <sup>9</sup> Blue Sky Spectroscopy Inc., Lethbridge, Alberta, Canada
- <sup>10</sup> *Herschel* Science Centre, ESAC, Madrid, Spain
- <sup>11</sup> European Space Astronomy Centre, Madrid, Spain
- <sup>12</sup> Instituto de Astrofísica de Andalucía (CSIC), Granada, Spain
- <sup>13</sup> University of Michigan, Ann Arbor, USA
- <sup>14</sup> CAB. INTA-CSIC Crta Torrejon a Ajalvir km 4. 28850 Torrejon de Ardoz, Madrid, Spain
- <sup>15</sup> LERMA, Observatoire de Paris, and Univ. Pierre et Marie Curie, Paris, France
- <sup>16</sup> SRON Netherlands Institute for Space Research, PO Box 800, Groningen, The Netherlands
- <sup>17</sup> Leiden Observatory, University of Leiden, The Netherlands
- <sup>18</sup> Joint ALMA Observatory, Santiago, Chile
- <sup>19</sup> University of Lethbridge, Canada
- <sup>20</sup> University of Cologne, Germany
- <sup>21</sup> University of Bern, Switzerland

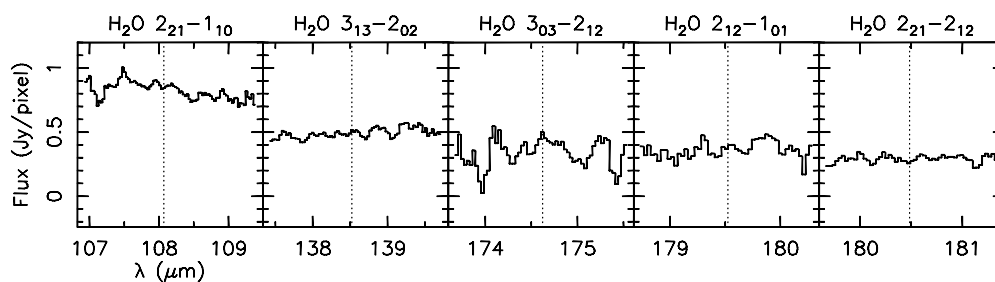


**Fig. 2.** Spectra of C/2006 W3 (Christensen) obtained with PACS on November 8, 2009 (central pixel pointed on the comet nucleus). The pixel size is  $9.4'' \times 9.4''$ . The wavelengths of water lines are indicated by vertical dashed lines.

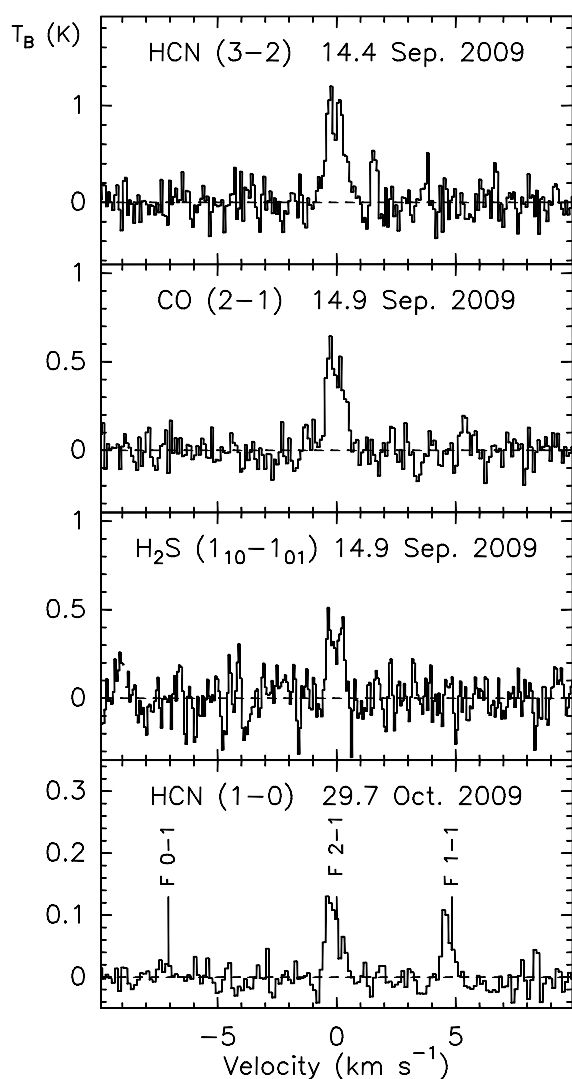


**Fig. 5.** Spectra of C/2006 W3 (Christensen) observed with the IRAM 30-m telescope.

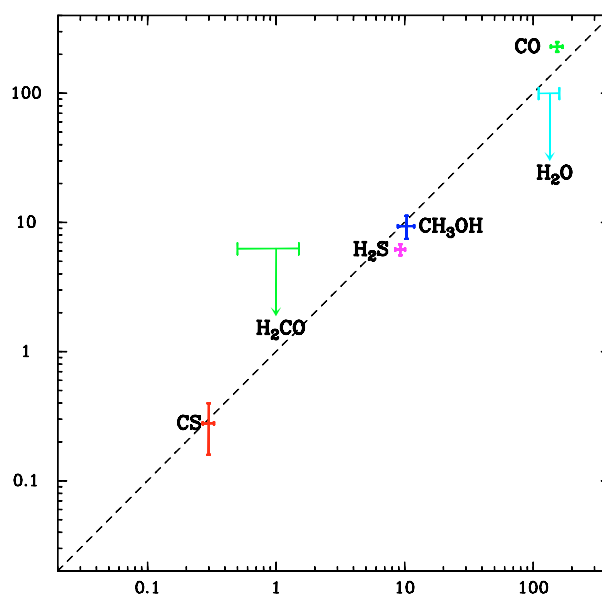


**Fig. 6.** Comparison of measured abundances relative to HCN in comets C/2006 W3 (Christensen) and C/1995 O1 (Hale-Bopp) at 3.3 AU from the Sun.